1)I am concerned about the use of the Granger causality method since this assumes linear dynamics and Gaussian statistics. The MJO is probably a non-linear phenomenon. Did you also test the convergent cross-mapping approach by Sugihara? In a recently published studies we have shown that time-lagged CCM and machine learning approaches are much better: Huang, Y., C. Franzke, N. Yuan and Z. Fu, C1 ESDD Interactive comment Printer-friendly version Discussion paper 2020: Systematic identification of causal relations in high-dimensional chaotic systems: Application to Stratopshere-Troposphere coupling. Clim. Dyn., in press. https://link.springer.com/article/10.1007/s00382-020-05394-0Huang, Y., Z. Fu and C. Franzke, 2020: Detecting causality from time series in a machine learning framework. Chaos, 30, 063116.

R: In this article, we have used the PDC method to infer Granger causality between multiple time-series in the frequency domain. The main advantage of PDC and Granger causality is that it is theoretically related to the mutual information rate (MIR) between signals (see Takahashi et. al 2010 Information theoretic interpretation of frequency domain connectivity measures.

Biological Cybernetics, v.103, p. 463-469, 2010.; Geweke, J. F. (1984). Measures of conditional linear dependence and feedback between time series. *Journal of the American Statistical Association*, *79*(388), 907-915.). Information-theoretic quantities are usually costly to estimate directly from time-series since it relies on the estimation of multi-dimensional probability distributions. As proved in Takahashi et. al 2010, PDC is a Gaussian approximation to the MIR. This means that if the time-series are stationary and Gaussian PDC provides an exact estimate for the MIR, when the time-series are not Gaussian (possibly due to underlying nonlinearities) the PDC will capture part but not all of the information flow between the time-series.

There are many "causality" estimation methods in the literature, all of them with some advantages and drawbacks. Among the several causality detection methods the Convergent-Cross Mapping (CCM) method is proposed as a method that is capable to capture couplings in highly-nonlinear settings since it relies phase-space embedding procedures. CCM. However, it comes with a few drawbacks that would require more in-depth investigation before we could apply it in the present setting, namely:

(1) CCM is a bi-variate measure. Granger causality and PDC are genuinely multivariate measures.

(2) CCM may lead to wrong or misleading results when moderate to high levels of noise are present (see Mønster, D., Fusaroli, R., Tylén, K., Roepstorff, A., & Sherson, J. F. (2017). Causal inference from noisy time-series data—Testing the Convergent Cross-Mapping algorithm in the presence of noise and external influence. *Future Generation Computer Systems*, *73*, 52-62.). Granger causality and PDC are designed to work for signals with stochasticity.

(3) CCM does not have an automated way to decide the optimal lag between time series. Granger causality and PDC are based on autoregressive process in which order estimation is well studied.

(4) There are no theoretical guarantees for the statistical properties of CCM. Both PDC and Granger causality are at very well studied measures in which there are thousands of articles applying it and we understand well their statistical properties (Lutkepohl, 2005; Takahashi et al., 2007).

Finally, although PDC is a stochastic linear method, it correctly reconstruct the topology of networks of nonlinear oscillators (see Winterhalder, M., Schelter, B., & Timmer, J. (2007). Detecting coupling directions in multivariate oscillatory systems. *International Journal of Bifurcation and Chaos*, *17*(10), 3735-3739.), Moreover, it has been successfully and extensively used to infer information flow in highly nonlinear time-series data in neuroscience (Bressler, S. L., & Seth, A. K. (2011). Wiener–Granger causality: a well established methodology. *Neuroimage*, *58*(2), 323-329.). The fact that PDC can detect nonlinear interactions is not difficult to understand, given that linear regression also can see nonlinear interaction unless the nonlinearity is highly non-monotonic.

2) It is not really clear to me how you compute the time series you then use for the analysis. Are these just the projections of particular normal modes? If yes, how many normal modes do you use to represent the MJO and QBO? Or do you use just one normal mode for the respective wave type?

R:The time-series associated with the normal modes that we used correspond the the energy of a group of modes defined by:

$$E(t) = \frac{1}{2} \sum_{m=1}^{M} gD_m \sum_{k=0}^{K} \sum_{n=0}^{N} ([\chi_{kmn}(t)]^* \chi_{kmn}(t))$$

Where g is the acceleration of gravity, D_m is the equivalent height of the m-th vertical index, $\chi_{kmn}(t)$ is the complex amplitude of the normal mode with zonal wave number k, meridional index n and vertical index m. M=43, K=32 and N are the respective truncation numbers for each index. For the MJO we selected the three first three even meridional indices for the Rossby modes (no selection on the vertical and zonal modes).

3) While the MJO normal modes have large amplitudes during MJO events and the set of normal modes are also then coherent. However, the normal modes can also have large amplitudes during non-MJO/QBO events. So, I think your results on the MJO time scale might be robust but I am not sure whether your results are related to the MJO on longer time scales; there probably is an effect of the QBO/ozone on the particular normal modes but I do not think you have shown that this is really related to the MJO.

In the present version of the manuscript we have included the composite analysis as suggested by this referee. This analysis clearly shows a difference in the long term behavior of the MJO-related modes, this was done for the QBO timescale (~28 months), and probably accounts for the causality between QBO modes and MJO modes at this time scale. Differences at other time-scales such as the solar cycle timescale still need to the investigated in more detail.

4) The quality of some of the figures is rather poor (Figs. 3, 10, 11).

R:Due to the large number of figures we were having problems compiling the file, which lead us to include figures with lower resolution, in the new version of the manuscript we included figures with better resolution.

 5) What do the diagonal plots in Fig. 1 represent? Is that the causality of the time series with itself? What can I learn from this?

R:The diagonal plots correspond to the power spectrum of each of the variables, which is equivalent to the PDC of between the variable and itself.

6) How do you compute the significance of the causal relations? A brief description would be useful.

R:In this version of the manuscript we have included a description of the statistics, in particular how we obtain the confidence intervals of the PDC. We refer back to our response to the first question of referee #1.

"We apologize that we did not describe the statistics with sufficient details. PDC is a function of the coefficients of vector autoregressive model. Given that the coeffcients are asymptotically jointly normally distributed, we can use the delta method (Serfling, 1980) to analytically calculate the asymptotic statistics for PDC. After a straighforward but tedious algebraic computation, we can show that PDC at frequency lambda is distributed asymptotically (under the null hypothesis of zero PDC) as the weighted sum of two chi-square with one degree of freedom (Takahashi et al., 2007). Therefore, we can use this asymptotic distribution to calculate the p-values. For details of the derivation, we refer to Takahashi et al. (2007).

Significance levels for frequency domain quantities are controled only point-wise as this is the standard everywhere. The reason for this is that the point estimates for neighboring frequencies are highly correlated. Therefore, standard correction like bonferroni or even FDR that assume independence or weak dependence give the wrong signficance level. Every single article that we found where PDC, coherence or bi-coherence were used and the signficance level is reported use the frequency-wise significance level (for representative examples see Huybers and Curry, 2006 and Came et al., 2007). For PDC it is easy to see that the use of frequency-wise significance level is reasonable given that the PDC values for different frequencies are the fourier transform of the same coefficents of the autoregressive process. The fact that lower frequency have fewer samples are taken care by higher threshold values for PDC at lower frequencies. We added the following brief description of the statistics for PDC in the main text.

"PDC is a function of the coefficients of vector autoregressive model. Given that the coeffcients are asymptotically jointly normally distributed, we can use the delta method (Serfling, 1980) to obtain analytically the asymptotic statistics for PDC. After na algebraic computation we can show that PDC at frequency lambda is distributed asymptotically (under the null hypothesis of zero PDC) as the weighted sum of two chi-square with one degree of freedom (Takahashi et al., 2007). Therefore, we can use the the asymptotic distribution to calculate the p-value. For details of the derivation, we refer to Takahashi et al. (2007). The significance level used in the article for PDC is the frequency-wise value as it is the standard for frequency domain analysis given the high

correlation between the point estimates for neighboring frequencies (see e.g. Huybers and Curry, 2006; Came et al., 2007)."

"

7) There is a recent paper: Franzke, C., D. Jelic, S. Lee and S. Feldstein, 2019: Systematic Decomposition of the MJO and its Northern Hemispheric Extra-Tropical Response into Rossby and Inertio-Gravity Components. Q. J. Roy. Meteorol. Soc., 145, 1147-1164. They use a composite approach which might be better suited to investigate the MJO and QBO. Using linear regression might mix too many non-events into the analysis. C2 ESDD Interactive comment Printer-friendly version Discussion paper.

R:In the present version of the manuscript we have included an analysis derived from the reference suggest by the referee "Systematic Decomposition of the MJO and its Northern Hemispheric Extra-Tropical Response into Rossby and Inertio-Gravity Components. Q. J. Roy. Meteorol. Soc., 145, 1147-1164.". We believe that this analysis has lead to a better understanding of how the QBO affects each normal mode component of the MJO (ROT and Kelvin). In what follows we include the corresponding figures with corresponding descriptions.
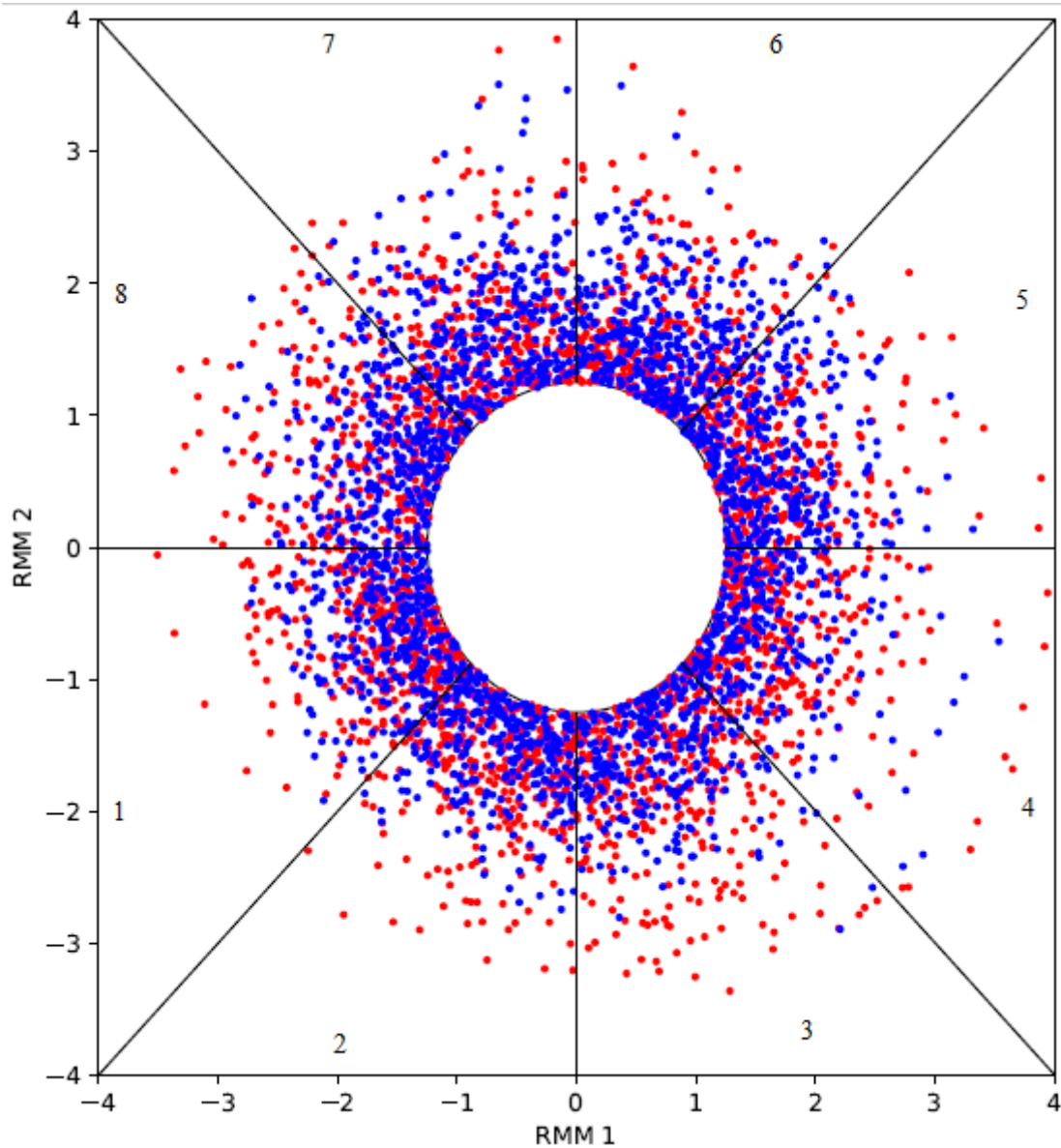
Figure 2.7.1: MJO phase diagram showing all points (days) in which $(RMM_1^2 + RMM_1^2 \geq 1)$. Points marked in red

In order to exclude the cases in which the RMM index is not associated with a MJO event we excluded all cases in which $(RMM_1^2 + RMM_1^2 < 1)$., among those cases we separated the ones for which the stratospheric zonal wind at 30Mb was positive (red) and negative (blue) in the figure 2.7.1. The MJO phase diagram was divided into 8 phases as in Franzke et. al 2019. For which QBO (positive or negative) state and for which MJO phase (i=1,2,…,8) we calculated the mean velocity and pressure fields associated with ROT and Kelvin modes at 200 Mb.

Figures 2.7.2 and 2.7.3 are display respectively the composites associated with the reconstructions of velocity and geopotential height fields associated with ROT modes for each of the 8 MJO phases with positive stratospheric zonal wind at 30 mb (SZW30+) and negative (SZW30+). In order to compare both composites we compute the difference

between SZW30+ and SZW30- of each field for each MJO phase. This is displayed in figure 2.7.4. We notice that for phases 1-3 the difference (of the geopotential height fields represented by the hatched region) is statistically significant for almost the entire domain. For phase 4 the fields are more similar with small regions with significant difference, associated with Rossby double vortices. Between phases 5-8 the areas with significant difference become larger again.
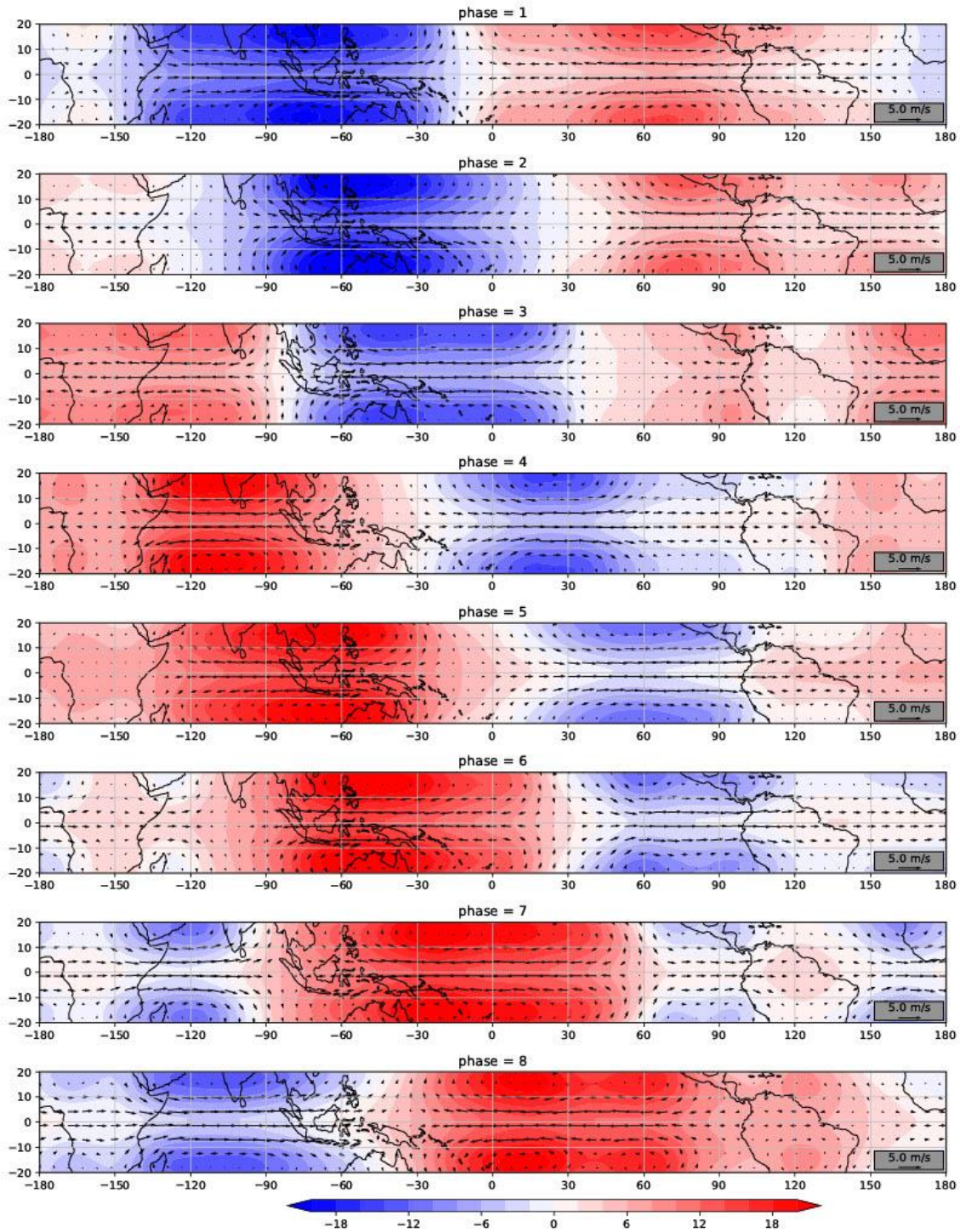

Figure 2.7.2: Reconstruction of the velocity and geopotential height fields associated with ROT modes with SZW30+ at 200 Mb.
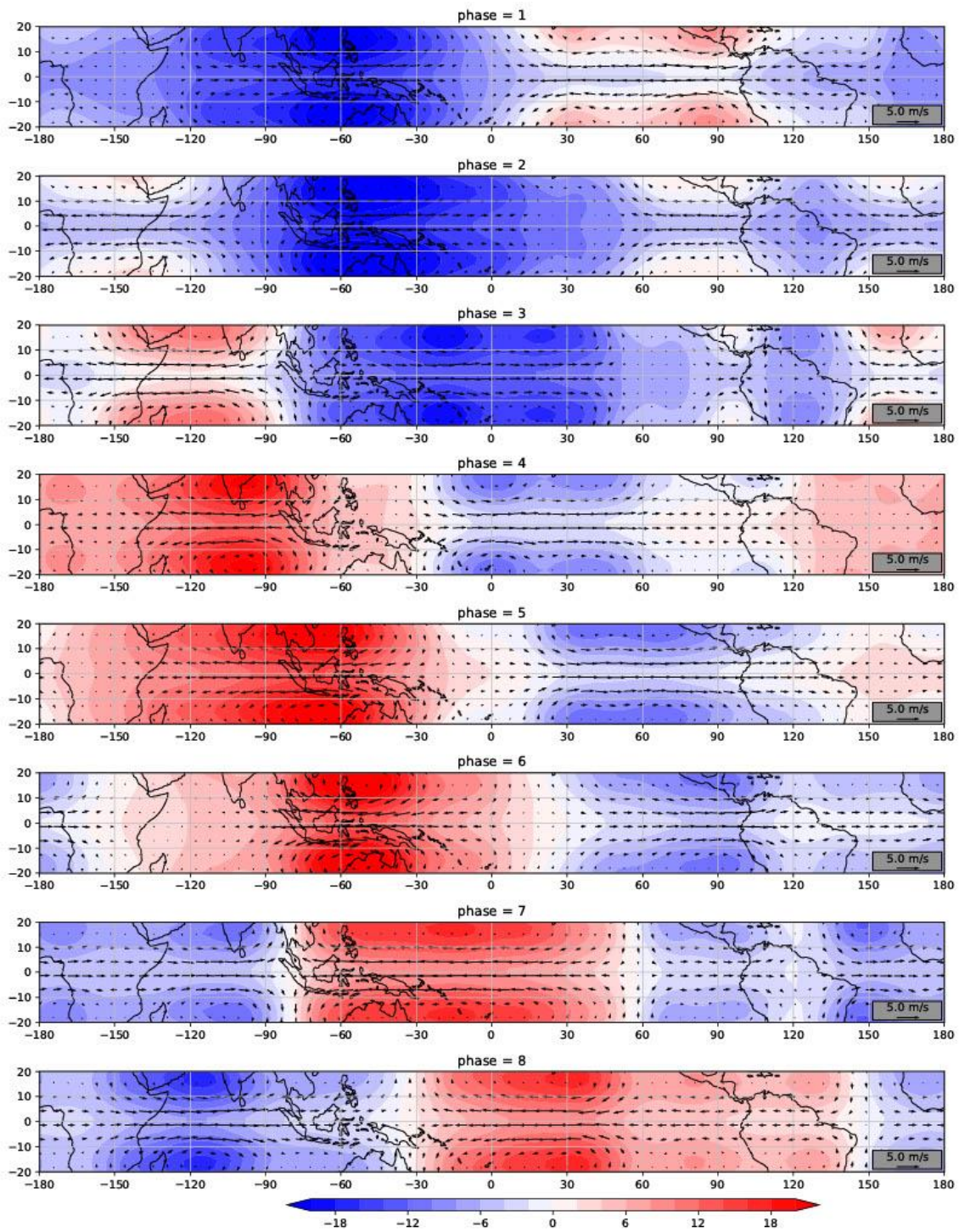
Figure 2.7.3: Reconstruction of the velocity and geopotential height fields associated with ROT modes with SZW30- at 200 Mb.
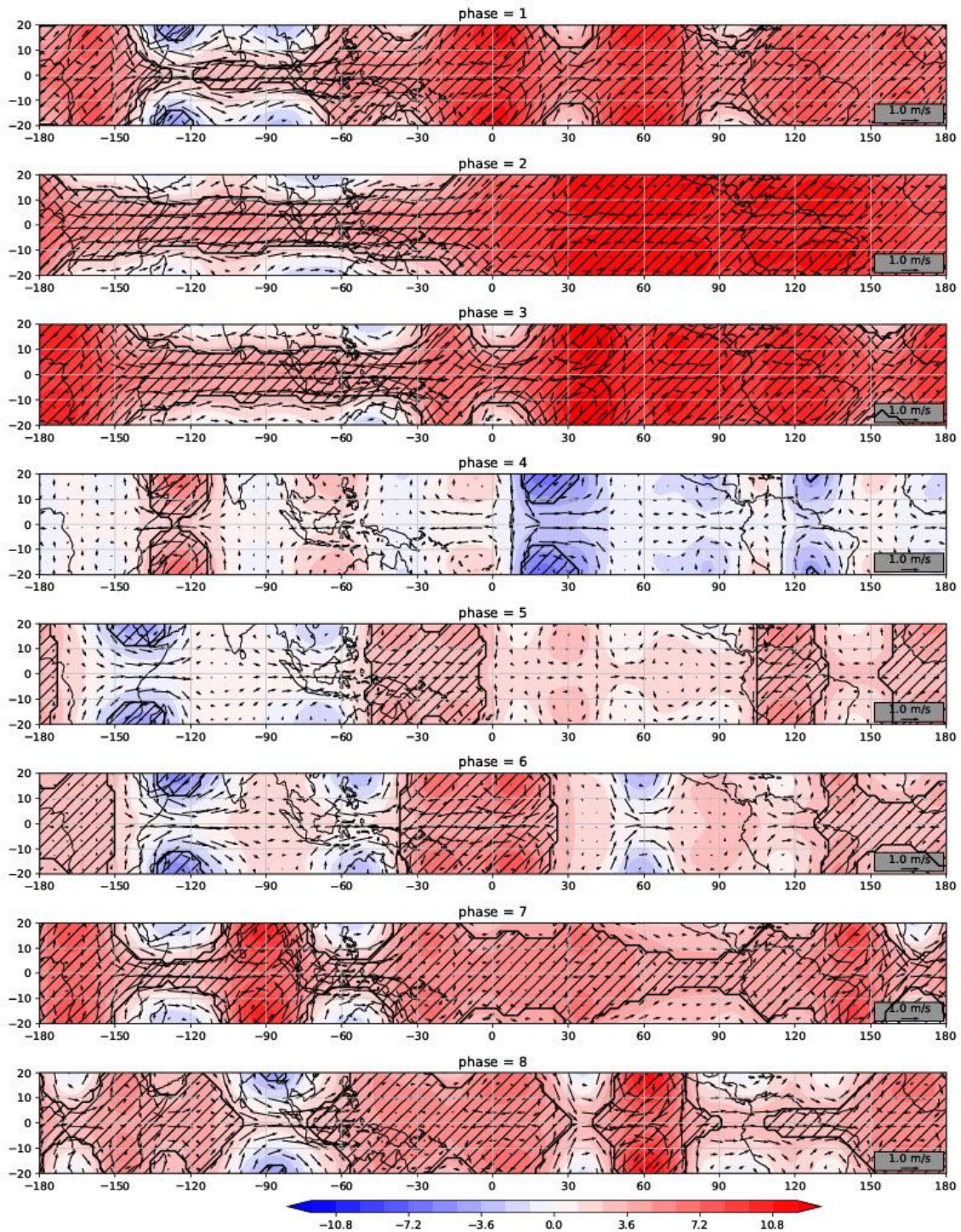
Figure 2.7.4: Difference between of the velocity and geopotential height fields associated with ROT modes with SZW30+ and SZW30-. The hatched region corresponds to significant difference of the geopotential height values under 5% confidence level.
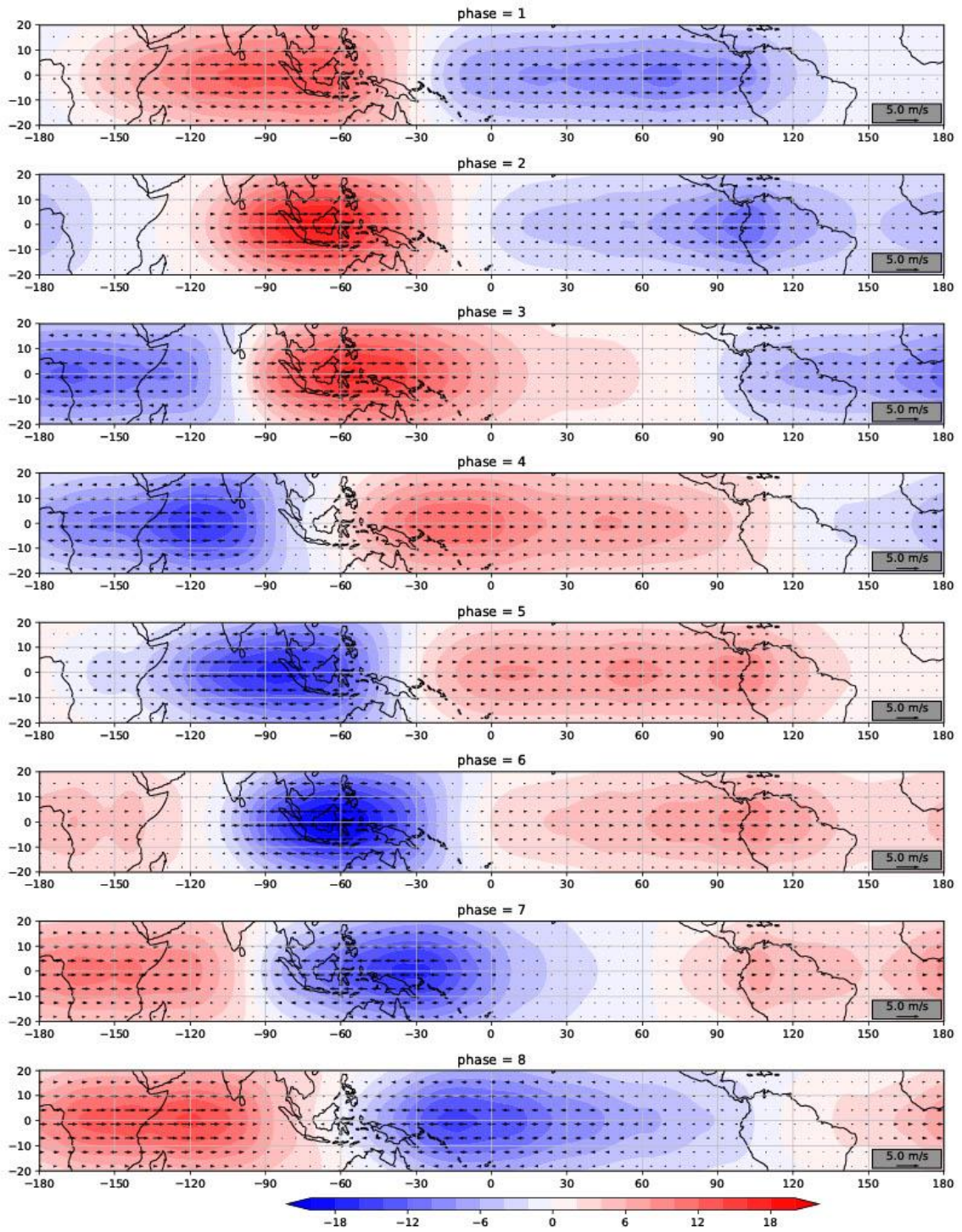
Figure 2.7.5: Reconstruction of the velocity and geopotential height fields associated with Kelvin modes with SZW30+ at 200 Mb.
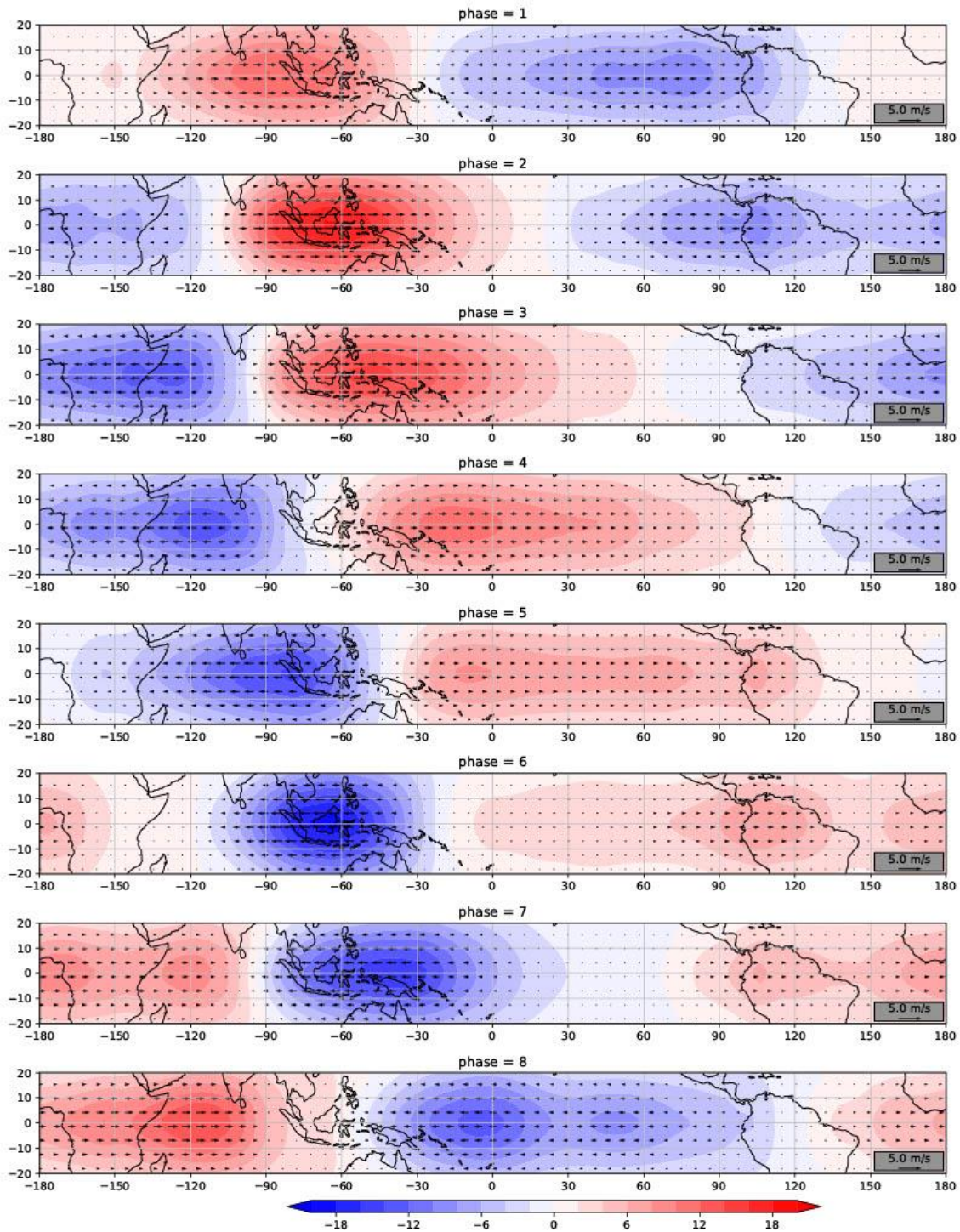
Figure 2.7.6: Reconstruction of the velocity and geopotential height fields associated with Kelvin modes with SZW30- at 200 Mb.

Figures 2.7.5 and 2.7.6 display respectively the composites associated with the reconstructions of velocity and geopotential height fields associated with the Kelvin mode for each of the 8 MJO phases with positive stratospheric zonal wind at 30 mb (SZW30+) and negative (SZW30+). In order to compare both composites we compute the difference between SZW30+ and SZW30- of each field for each MJO phase. This is

displayed in figure 2.7.7. We notice that for phases 1-3 the difference (of the geopotential height fields represented by the hatched region) is statistically significant for almost the entire domain. Unlike in the case of ROT modes, for the Kelvin modes the distribution of statistically significant difference is more even throughout a MJO cycle with a larger area on phase 2 and more similar fields on phase 4. It is possible to notice a propagation pattern with negative geopotential height anomaly beginning at phase 4 and ending at phase 7.
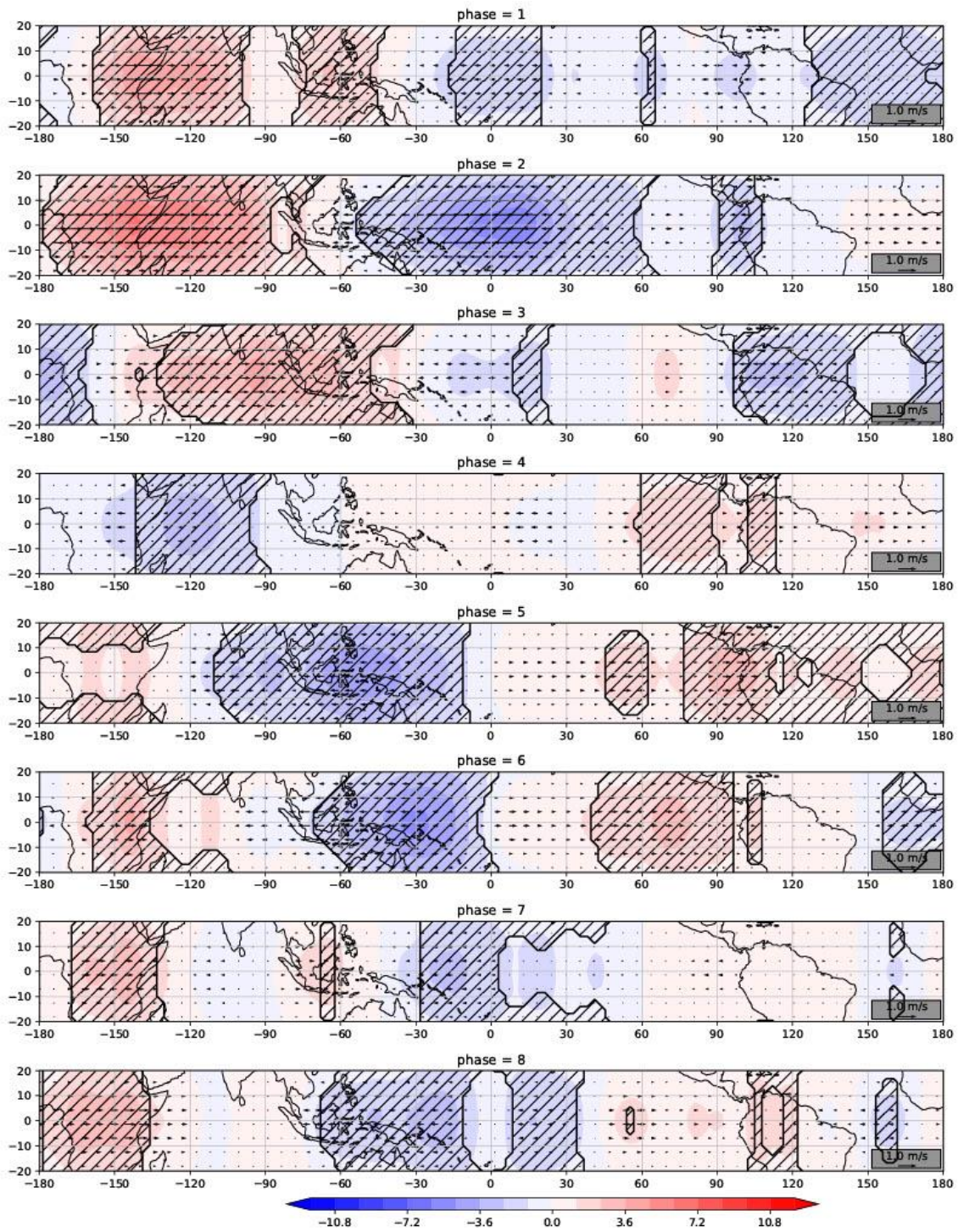
Figure 2.7.7: Difference between of the velocity and geopotential height fields associated with Kelvin modes with SZW30+ and SZW30-. The hatched region corresponds to significant difference of the geopotential height values under 5% confidence level.

8) Please correct "Frankze" to "Franzke" in the references.

The correction was made.